J. Fluid Mech. (1977), *vol.* 79, *part* 2, *pp.* 337–359
Printed in Great Britain

Spectral energy transfer in high Reynolds number turbulence

By K. N. HELLAND, C. W. VAN ATTA
Department of Applied Mechanics and Engineering Sciences
University of California, La Jolla
AND G. R. STEGEN
Department of Civil Engineering, Colorado State University, Fort Collins†

(Received 17 February 1976 and in revised form 5 August 1976)

The spectral energy transfer of turbulent velocity fields has been examined over a wide range of Reynolds numbers by experimental and empirical methods. Measurements in a high Reynolds number grid flow were used to calculate the energy transfer by the direct Fourier-transform method of Yeh & Van Atta. Measurements in a free jet were used to calculate energy transfer for a still higher Reynolds number. An empirical energy spectrum was used in conjunction with a local self-preservation approximation to estimate the energy transfer at Reynolds numbers beyond presently achievable experimental conditions.

Second-order spectra of the grid measurements are in excellent agreement with local isotropy down to low wavenumbers. For the first time, one-dimensional third-order spectra were used to test for local isotropy, and modest agreement with the theoretical conditions was observed over the range of wavenumbers which appear isotropic according to second-order criteria. Three-dimensional forms of the measured spectra were calculated, and the directly measured energy transfer was compared with the indirectly measured transfer using a local self-preservation model for energy decay. The good agreement between the direct and indirect measurements of energy transfer provides additional support for both the assumption of local isotropy and the assumption of self-preservation in high Reynolds number grid turbulence.

An empirical spectrum was constructed from analytical spectral forms of von Kármán and Pao and used to extrapolate energy transfer measurements at lower Reynolds number to $R_\lambda = 10^5$ with the assumption of local self preservation. The transfer spectrum at this Reynolds number has no wavenumber region of zero net spectral transfer despite three decades of $k^{-\frac{5}{3}}$ behaviour in the empirical energy spectrum. A criterion for the inertial subrange suggested by Lumley applied to the empirical transfer spectrum is in good agreement with the $k^{-\frac{5}{3}}$ range of the empirical energy spectrum.

† Present address: Science Applications, Inc., 8400 W. Park Dr., McLean, Washington.

1. Introduction

The nonlinear dynamics of spectral energy transfer has been a central problem in turbulence research. Early theoretical efforts which ignored the third-order velocity correlations have generally been abandoned and attempts to describe turbulent flows usually model the most important, if not all, nonlinear terms. Many attempts have been made to predict the form of the energy spectrum by closing the system of governing equations with *ad hoc* hypotheses. The approach is one of reasoned physical and dimensional arguments to determine the relationship between the spectral energy transfer and the energy spectra. The hypothesis closes the governing differential equations, and the resulting energy spectrum is compared with measurements. The procedure is appealing because it offers the possibility of providing insight into the physical nature of the energy-transfer process. On the other hand, the interaction mechanisms modelled by the hypothesis cannot be tested directly, and the energy spectrum is often insensitive to the closure model.

The first successful measurements of the net energy transfer spectrum were made by Uberoi (1963), who measured the energy decay and dissipation spectra in grid turbulence and inferred the energy transfer spectrum indirectly under the assumption of isotropy. Van Atta & Chen (1969) used fast Fourier transform methods to derive the net energy transfer spectrum directly from measurements of the third-order velocity correlations.† They obtained good agreement between direct and indirect measurements of the energy transfer spectrum, thus verifying the assumption of local isotropy at third order. Yeh & Van Atta (1973) simplified the direct calculation technique of Van Atta & Chen and extended the measurements to scalar energy transfer spectra.

The studies referred to above have emphasized measurements of the net energy transfer spectra in grid turbulence. However, the net energy transfer spectrum is a limited end in itself, for it represents only the net transfer of energy into or out of each wavenumber. It gives no information about the nonlinear interactions among arbitrarily separated wavenumbers. Yeh & Van Atta (1973) described schematically the very complicated measurements which would be necessary to obtain information about wavenumber–wavenumber energy transfer. The required measurements appear impractical for the time being, but the present investigation as well as those in the past should be viewed as preliminary steps necessary before a multi-wavenumber energy transfer spectrum could be measured.

In the present investigation the net energy transfer spectrum is calculated from experimental data at Reynolds numbers significantly larger than those of previous investigators. High Reynolds number measurements in both a decaying grid flow and a large free jet are used. The analysis of grid data obtained by one of us (GRS) at Colorado State University (CSU) forms the major part of this investigation. In addition, data from a very high Reynolds number jet obtained by C. A. Friehe and associates at the University of California, San

† The term 'net energy transfer' is used here to mean the net gain or loss of kinetic energy at a wavenumber k from all other wavenumbers.

Diego (UCSD), are used to combine an investigation of energy transfer at an even higher Reynolds number with direct calculations of the energy transfer spectrum in a shear flow. The analysis of both grid and jet flows provides an opportunity to compare the energy transfer calculations in a nearly isotropic flow with those in a shear flow containing a large range of anisotropic wavenumbers. The validity of the isotropic assumption for the CSU grid data is tested using second-order spectral techniques, and for the first time one-dimensional third-order isotropic spectral relations are used as a higher-order isotropy test analogous to the usual second-order methods.

2. Problem formulation

The equations appropriate to homogeneous, isotropic, decaying grid turbulence are reviewed in this section. Derivations of these equations may be found in Batchelor (1953, chap. 3) and Hinze (1959, chap. 3), and various forms of the energy transfer spectra are discussed in Yeh & Van Atta (1973). The isotropic equation for the decay of the three-dimensional energy spectrum $E(k)$ is

$$\partial E(k)/\partial t = T(k) - 2\nu k^2 E(k), \tag{2.1}$$

where each term is related to a measurable one-dimensional spectrum. The function $T(k)$ is the net three-dimensional energy transfer spectrum representing the balance of energy transfer into the wavenumber k from all other wavenumbers. Pressure does not appear explicitly in (2.1) because of the incompressibility assumption. The terms in (2.1) are not directly measurable, and the relationship of each term to an isotropically related, one-dimensional, measurable spectrum is summarized in this section.

The three-dimensional energy spectrum $E(k)$, sometimes referred to as the 'wavenumber-magnitude' spectrum, is related to the one-dimensional total energy spectrum $\phi_{ii}(k_1)$ by

$$E(k) = -k_1 d\phi_{ii}(k_1)/dk_1, \tag{2.2}$$

where k and k_1 are interchangeable in a spherically symmetric isotropic representation. The summation convention implies

$$\phi_{ii}(k_1) = \phi_{11}(k_1) + \phi_{22}(k_1) + \phi_{33}(k_1) \tag{2.3}$$

and application of isotropic relations yields

$$\phi_{22}(k_1) = \phi_{33}(k_1) \tag{2.4}$$

and

$$\phi_{22}(k_1) = \tfrac{1}{2}[\phi_{11}(k_1) - k_1 d\phi_{11}(k_1)/dk_1]. \tag{2.5}$$

Measurement in an isotropic flow of either $\phi_{11}(k_1)$ alone or both $\phi_{11}(k_1)$ and $\phi_{22}(k_1)$ permits the calculation of $\phi_{ii}(k_1)$ and, therefore, the three-dimensional spectrum $E(k)$.

The one-dimensional spectrum $\phi_{ii}(k_1)$ is related to the second-order correlation by

$$\phi_{ii}(k_1) = (2\pi)^{-1} \int_{-\infty}^{\infty} R_{i,i}(r_1) \exp\{-ik_1 r_1\} dr_1 = \Delta k \langle U_i^*(k_1) U_i(k_1) \rangle, \tag{2.6}$$

where * denotes the complex conjugate and

$$U_i(k_1) \equiv \int_{-\infty}^{\infty}\int_{-\infty}^{\infty} U_i(k_1, k_2, k_3)\, dk_2\, dk_3$$
$$\equiv (2\pi)^{-1}\int_{-\infty}^{\infty} u_i(x_1, 0, 0)\exp\{-ik_1x_1\}\, dx_1 \tag{2.7}$$

is the one-dimensional Fourier transform of $u_i(x_1)$. The integral of (2.2) is

$$2\int_0^{\infty} E(k)\, dk = \int_{-\infty}^{\infty} \phi_{ii}(k_1)\, dk_1 = \langle u_i u_i\rangle, \tag{2.8}$$

where $\langle u_i u_i\rangle = q^2$ is twice the total kinetic energy. Note that the definitions of $\phi_{ii}(k_1)$ and $E(k)$ used here differ from those of some authors who include a factor of 2 within the definition of ϕ_{ii} and E. The three-dimensional dissipation spectrum is defined by

$$D(k) = 2\nu k^2 E(k). \tag{2.9}$$

The net transfer spectrum $T(k)$ is related to measurable one-dimensional spectral forms in much the same way as the energy spectrum $E(k)$ described above. The three-dimensional energy transfer spectrum is related to a one-dimensional total energy transfer spectrum $S_{1i,\,i}(k_1)$ by

$$T(k) = -4\{k_1 S_{1i,\,i}(k_1)\} + 2k_1\, d\{k_1 S_{1i,\,i}(k_1)\}/dk_1, \tag{2.10}$$

where k and k_1 are again interchangeable in a spherically symmetric isotropic representation. The summation convention implies

$$S_{1i,\,i}(k_1) = \mathrm{Im}\{S_{11,\,1}(k_1) + S_{12,\,2}(k_1) + S_{13,\,3}(k_1)\} \tag{2.11}$$

and after using the isotropic condition, the relationships among the individual transfer spectra are

$$S_{13,\,3}(k_1) = S_{12,\,2}(k_1), \tag{2.12}$$

$$\mathrm{Im}\{S_{12,\,2}(k_1)\} = \tfrac{1}{4}[\mathrm{Im}\{S_{11,\,1}(k_1)\} - k_1\, d\,\mathrm{Im}\{S_{11,\,1}(k_1)\}/dk_1]. \tag{2.13}$$

These third-order expressions are analogous to those among the energy spectra. The one-dimensional transfer spectrum is equivalent to the Fourier transform of the two-point third-order correlation

$$S_{1i,\,i}(k_1) = (2\pi)^{-1}\int_{-\infty}^{\infty} R_{1i,\,i}(r_1)\exp\{-ik_1r_1\}\, dr_1, \tag{2.14}$$

which after application of the convolution theorem becomes

$$S_{1i,\,i}(k_1) = \Delta k\,\langle U_{1i}^*(k_1)\, U_i(k_1)\rangle, \tag{2.15}$$

where the additional measurable Fourier transform is defined by

$$U_{1i}(k_1) = (2\pi)^{-1}\int_{-\infty}^{\infty} u_1(x_1, 0, 0)\, u_i(x_1, 0, 0)\exp\{-ik_1x_1\}\, dx_1. \tag{2.16}$$

The definitions of the Fourier transforms in (2.7) and (2.16) apply to the instantaneous velocity field as well as to the averaged spectral quantities.

One additional assumption is made to permit simple evaluation of the Fourier transforms of (2.7) and (2.16): time and space are related using the frozen-flow hypothesis of Taylor. This assumption has been checked for grid turbulence experimentally by Favre, Gaviglio & Dumas (1955) using correlation functions and by Stegen & Van Atta (1970) using cross-spectral analysis.

3. Experimental data

Grid turbulence

The measurements of grid turbulence were made at CSU by one of us (GRS) in a closed-circuit wind tunnel with a $1{\cdot}8 \times 1{\cdot}8 \times 24{\cdot}3$ m test section. A biplanar grid with a square mesh ($M = 22{\cdot}9$ cm) and square rods (3·81 cm) was located one tunnel diameter downstream from the entrance to the test section. The tunnel was operated at a mean speed of 2900 cm/s, giving a grid Reynolds number of 410 000. A cooling system was required to provide steady conditions, and the resulting temperature at the operating speed was 1 °C. The mean velocity ($\overline{U}$) and velocity fluctuations in the longitudinal (u_1) and transverse (u_2) directions were measured at downstream locations of $X/M = 35$, 38 and 41, where X is the distance from the grid. All detailed calculations in the present study were made at $X/M = 38$. Additional details of the experimental conditions are given by Schedvin, Stegen & Gibson (1974).

The fluctuating velocities were measured with an X-wire array (Thermo-Systems, Inc. Model 1241-T1.5). The sensors were operated in the constant-temperature mode using DISA Model 55D01 hot-wire anemometer systems and were linearized with DISA Model 55D10 linearizers. Sum and difference amplifiers were used to obtain voltage signals proportional to u_1 and u_2. The velocity fluctuations and their time derivatives generated by electronic differentiation were recorded on an Ampex FR1300 FM tape recorder at a speed of 60 in./s. The analog tapes were played back at UCSD on a Sangamo 3500 FM tape recorder at a speed of 7·5 in./s (8:1 speed reduction) to accommodate the maximum obtainable sample rate of the AMES digitizer system. The velocity fluctuations were low-pass filtered (cut-off at 14 400 Hz, real time), sampled with an analog-to-digital convertor at a rate of $f_s = 33370$ samples/s (real time) and recorded on digital tape with 12 bit resolution.

The Kolmogorov frequency estimated from $f_k = \overline{U}/2\pi\eta$, where η is the Kolmogorov length scale, was about 20 900 Hz. The calculations of Schedvin *et al.* (1974) with nearly identical data from this experiment show that the -3 dB point due to finite hot-wire attenuation of the energy spectrum occurs at a frequency of about 3700 Hz. In view of the large difference between the Kolmogorov frequency and the half-power frequency due to finite wire length the low-pass filter was set at 14 400 Hz, and the data were digitized with a Nyquist frequency of 16 680 Hz. This provided an optimum trade-off between adequate sampling bandwidth and frequency resolution $\Delta f = 1/N\,\Delta t$, where N is the number of samples in the discrete Fourier transform and $\Delta t = 1/f_s$ is the sampling interval. The transform sample size N was chosen to be 4096, giving a resolution of $\Delta f = 8{\cdot}15$ Hz.

	CSU grid	UCSD jet
X/M	38	60·5†
M (cm)	22·9	29·2†
$\overline{U}$ (cm/s)	2900	362
Re_M	410 000	800 000‡
ν (cm²/s)	0·162	0·155
ϵ (cm²/s³)	17 800	23 900
R_λ	237	951
η (cm)	0·022	0·0199
v_k (cm/s)	7·32	7·80
q^2/v_k^2	184	736
L/η	617	4900
α	1·51	1·3

† Based on jet exit diameter D.
‡ Based on jet exit velocity $\overline{U}_0$ and diameter D.

TABLE 1. Physical parameters for CSU grid and UCSD jet measurements.

Axisymmetric jet turbulence

The measurements of jet turbulence were made in the UCSD gymnasium by C. Friehe and coworkers and kindly lent to us for this study. A large vaneaxial fan manufactured by Joy was supported with its centre-line 4·60 m above the floor. The fan had an exit diameter of 29·2 cm and was operated with an exit velocity $\overline{U}_0$ of 40 m/s, giving a jet Reynolds number $Re_D = \overline{U}_0 D/\nu$ of 800 000. The mean velocity $\overline{U}$ and the longitudinal fluctuating velocity u_1 were measured on the jet centre-line at an X/D of 60·5, where X is the distance from the jet exit plane.

The longitudinal velocity was measured with a single hot-wire probe (Thermo-Systems, Inc., Model 1210-T1.0) with a special short ($l_w = 0{\cdot}5$ mm), small diameter ($d_w = 0{\cdot}002\,54$ mm) sensor to minimize effects of finite wire length. The sensor was operated in the constant-temperature mode using a DISA Model 55A01 hot-wire anemometer and linearized with a DISA Model 55D10 linearizer. The velocity signal was recorded with a Sangamo Model 3500 FM tape recorder at 60 in./s. The analog signal was played back through a low-pass filter set at 4 kHz, digitally sampled at a rate of $f_s = 8340$ Hz and recorded on digital tape with 12 bit resolution. The Kolmogorov frequency was about 2900 Hz. The transform size N was 4096, giving a frequency resolution of $\Delta f = 2.04$ Hz. The parameters for the grid and jet flows are given in table 1.

4. Experimental results for CSU grid

One-dimensional second-order spectra

The measured transverse spectrum ϕ_{22} is compared with the transverse spectrum determined from the isotropic relation (2.5) and the measured longitudinal spectrum ϕ_{11} in figure 1. The first moment of the spectrum is used to emphasize the intermediate and high wavenumbers, which are expected to be the most nearly isotropic. The agreement between measured and calculated spectra is good

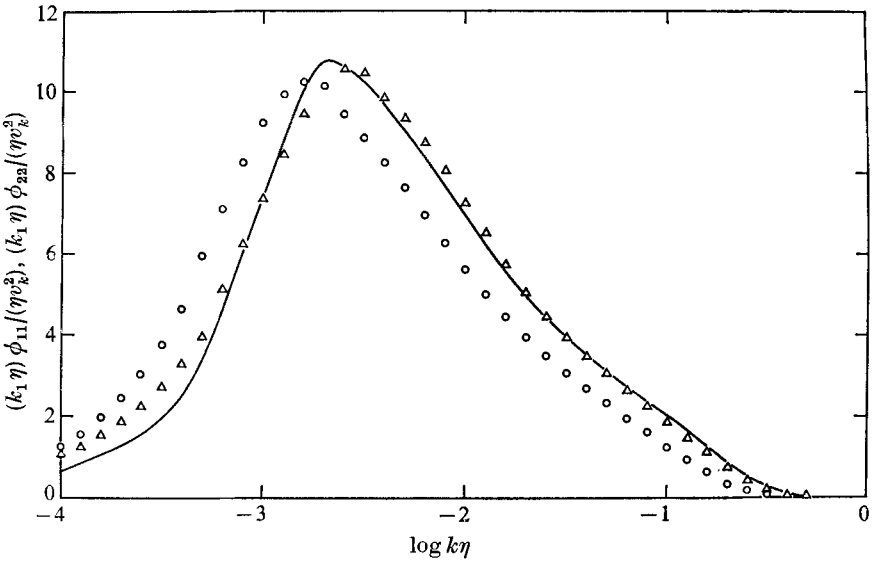

FIGURE 1. Comparison of measured and derived second-order spectra for CSU grid. ○, ϕ_{11}; △, ϕ_{22}; ——, ϕ_{22} derived from ϕ_{11} by isotropy [equation (2.5)].

down to a wavenumber of $\log k_1\eta \approx -3{\cdot}2$. The extent of isotropy found in the CSU data is much larger than that found by Kistler & Vrebalovich (1966) for grid turbulence at similar grid Reynolds numbers. These results are in good agreement with the spectral analysis of the CSU grid data by Schedvin *et al.* (1974), who applied the energy spectral test for isotropy to a separate set of data obtained at CSU under nearly the same operating conditions. Schedvin *et al.* also compare in detail the CSU grid measurements with the measurements of Kistler & Vrebalovich.

The total one-dimensional energy spectrum ϕ_{ii} is calculated from ϕ_{11} and the isotropic relations (2.3) and (2.5), and the one-dimensional total energy decay spectrum $\partial\phi_{ii}/\partial t$ is calculated from the ϕ_{ii} spectrum using an assumption of local self-preservation. The wire-length correction determined for the CSU data by Schedvin *et al.* (1974) was applied to the ϕ_{11} spectrum for this investigation. Previous investigators have been able to estimate the energy decay spectrum directly by measuring energy spectra at several downstream locations and using the approximation

$$\frac{\partial\phi_{ii}}{\partial t} \approx \overline{U}\frac{\Delta\phi_{ii}}{\Delta x} = \overline{U}\phi_{ii}\frac{\Delta\ln\phi_{ii}}{\Delta x} \tag{4.1}$$

at each wavenumber. Unfortunately (4.1) could not be used for either the CSU grid data or the UCSD jet data. Measurements of the CSU grid turbulence were made at a number of closely spaced values of X/M, but the decay of energy between measurement points was too small to permit accurate use of (4.1).

A self-preservation assumption was used to estimate energy decay spectra for the CSU grid and UCSD jet data to allow comparison of indirect estimates of

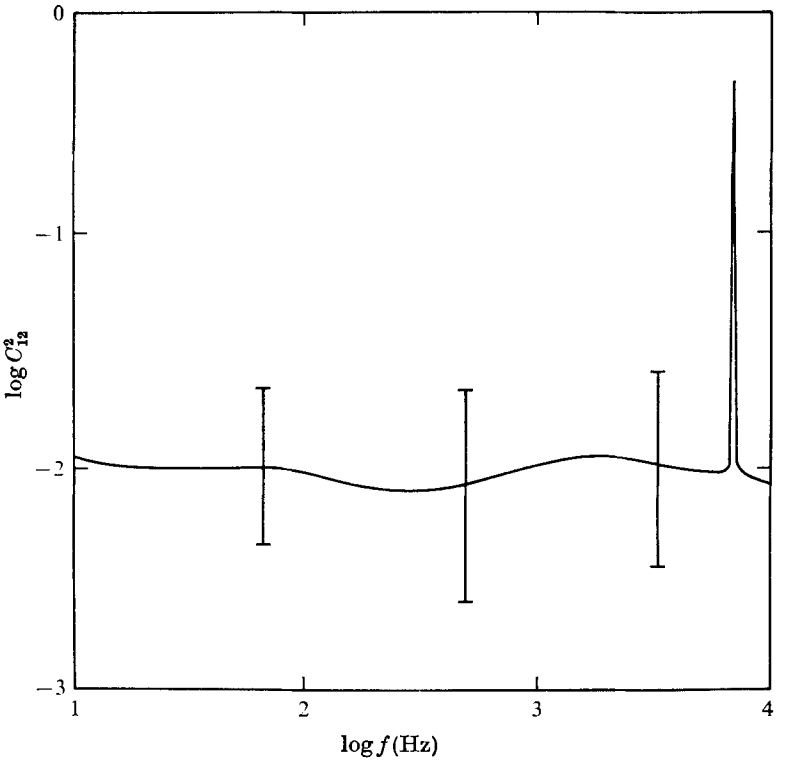

FIGURE 2. Squared coherence between velocities u_1 and u_2 for CSU grid measurements. Bars denote peak-to-peak variation of the measurements.

the energy transfer spectra with the direct Fourier calculations. The resulting decay spectrum can be expressed in terms of local quantities to give

$$\frac{\partial \phi_{ii}}{\partial t} = -\phi_{ii}\left(1 - \frac{d\ln \phi_{ii}}{d\ln k_1}\right)\frac{v_k^3}{q^2\eta} \tag{4.2}$$

for the spectral decay of the total one-dimensional spectrum appropriate for grid turbulence. The decay constant $v_k^3/q^2\eta$ is obtained from the measured spectrum, where v_k is the Kolmogorov velocity scale. Equation (4.2) provides a method of testing the assumption of local self-preservation in the wavenumber domain. Equation (4.2) was tried for the grid-turbulence data of Uberoi (1963), Van Atta & Chen (1969), and others, and the results reported by Helland (1974) show that the approximation of self-preservation can provide a good estimate of the energy decay spectrum in grid turbulence. The assumption of isotropy does not apply below a certain wavenumber; in particular, for the CSU data it ceases to apply below $\log k\eta \approx -3{\cdot}2$ according to the results in figure 1. Forcing the decay spectrum to satisfy this constraint may introduce errors in calculations performed at large wavenumber owing to the failure of isotropy at small wavenumber as pointed out by Van Atta & Chen in their discussion of the indirect calculations by Uberoi of transfer spectra.

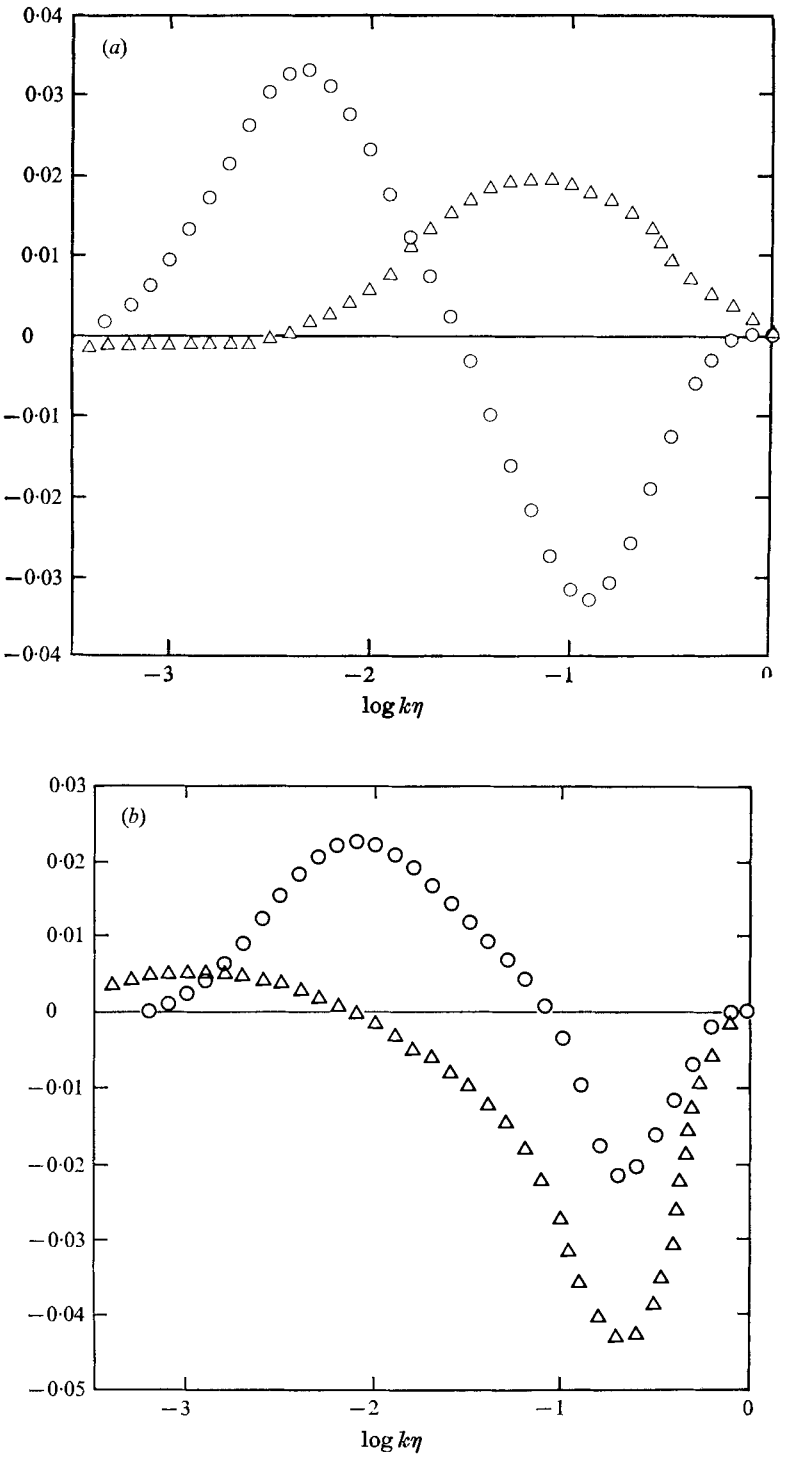

FIGURE 3. One-dimensional complex third-order spectra for CSU grid measurements. ○, imaginary part ; △, real part. (*a*) $(k_1\eta)^2 S_{11,1}/(v_k^3/\eta)$, (*b*) $(k_1\eta)^2 S_{12,2}/(v_k^3/\eta)$.

The coherence between the velocities u_1 and u_2 is presented in figure 2. The coherence is uniformly small for all wavenumbers except for a 7 kHz noise spike. For truly isotropic turbulence the coherence should be identically zero, but the small measured value is consistent with nearly isotropic turbulence. While the coherence function must be small for approximate validity of isotropy, there is no quantitative criterion which permits an objective determination of the approach to isotropy. For the CSU grid data, the coherence remains small and shows no tendency to increase at small wavenumber as it did, for instance, in the coherence measurements of velocity and temperature in the grid data of Yeh & Van Atta (1973). The residual coherence between u_1 and u_2 may be an indication of cross-talk in the X-wire array, or it may signify real deviations from isotropy. It is not possible to determine which without additional measurements. We suggest, for example, that X-wire measurements in a shear flow at the same Reynolds number would help to determine whether the finite coherence obtained in grid turbulence is a result of anisotropy or cross-talk. We expect that in a shear flow the approach to isotropy would be significantly reduced in comparison with grid turbulence. This is confirmed by Pierce (1972), who reports a coherence of 0·04 between $\partial u_1/\partial t$ and $\partial u_2/\partial t$ in a turbulent jet, significantly higher than the coherence of 0·01 reported herein for the CSU grid measurements. Note that coherence between velocity derivatives must be identical to that for the velocities themselves. Since coherence is non-dimensional, the properties of the Fourier transforms of derivatives result in cancellation of the multiplicative frequency factors which appear in the transforms of the derivatives.

One-dimensional third-order spectra

The complex one-dimensional longitudinal third-order cross-spectrum $S_{11,1}$ is presented in figure 3 (*a*). The real part of the spectrum is small compared with the imaginary part at low wavenumber, but at high wavenumber the real and imaginary parts are of the same order of magnitude. This is an apparent contradiction of the assumption of isotropy, which requires the real parts of the third-order cross-spectra to be zero. The condition is easy to see when one recalls that the reflexion condition of isotropy requires that a third-order correlation, say $\langle u_1(x)\, u_1^2(x+r)\rangle$, be antisymmetric in r about the origin for all lags r. The properties of the Fourier transform of an odd real function then require that the real part of the corresponding transform, the cospectrum of u_1 with u_1^2, be zero for all wavenumbers. It is not known how small the real part must be to remain approximately consistent with isotropy, in analogy with the problem encountered in interpreting the coherence between u_1 and u_2 in the previous subsection. The complex one-dimensional mixed longitudinal and transverse third-order cross-spectrum $S_{12,2}$ is presented in figure 3 (*b*). Again the real and imaginary parts are of the same order of magnitude for large wavenumbers.

Analytical forms for wire-length corrections for higher-order spectra are not available and hence cannot be applied to the measured higher-order spectra at the present time. However, since $T(k)$ is calculated both directly without wire-length corrections and indirectly with wire-length corrections, some estimate can

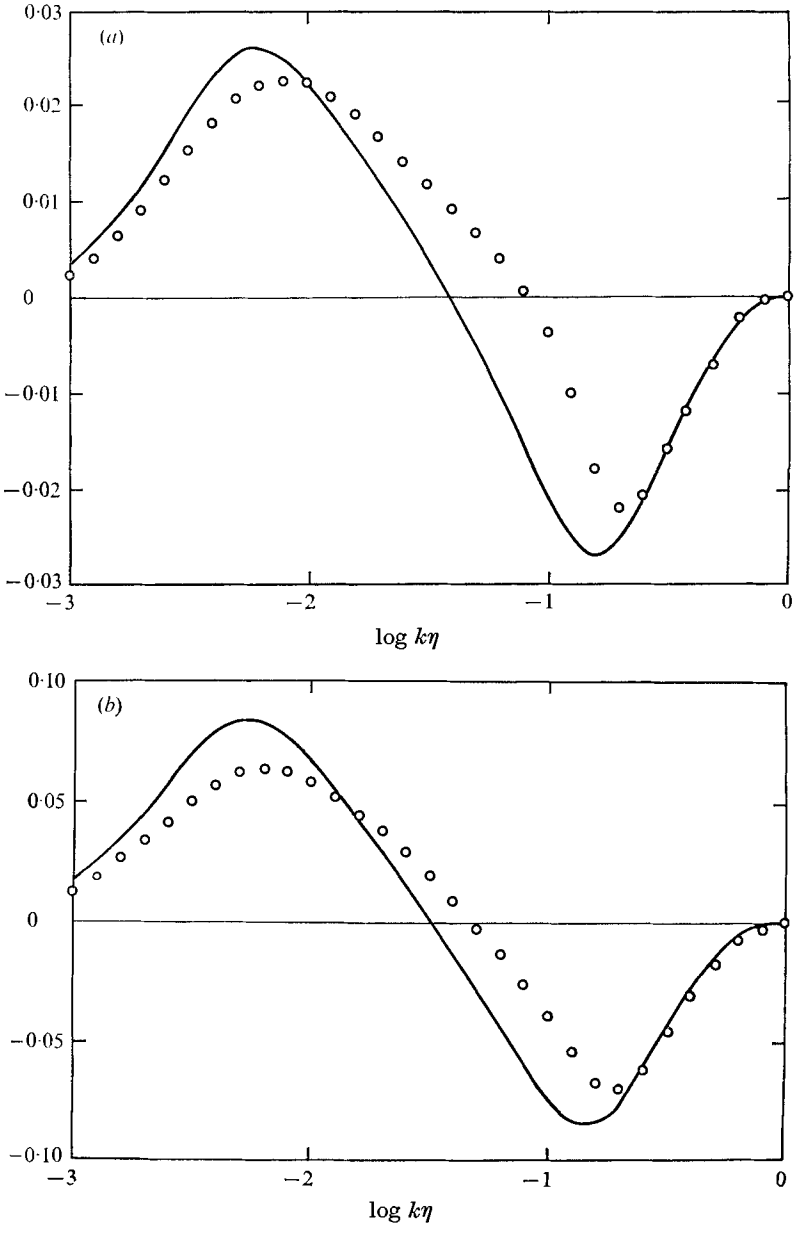

FIGURE 4. Comparison between measured and derived one-dimensional third-order spectra for CSU grid. ○, measured; ——, derived from Im $\{k_1^2 S_{11,1}\}$ by isotropy [(2.12) and (2.13)]. (*a*) Im $\{k_1^2 S_{12,2}\}$, (*b*) $k_1^2 S_{1i,i}$.

be made of the errors due to finite wire length, but further discussion will be postponed until the calculations for $T(k)$ have been presented.

In figure 4 (*a*) the isotropic test implied by (2.13) is applied to the measured and calculated third-order cross-spectrum Im $S_{12,2}$. The agreement is excellent at the lowest and highest wavenumbers with only moderate agreement at the inter-

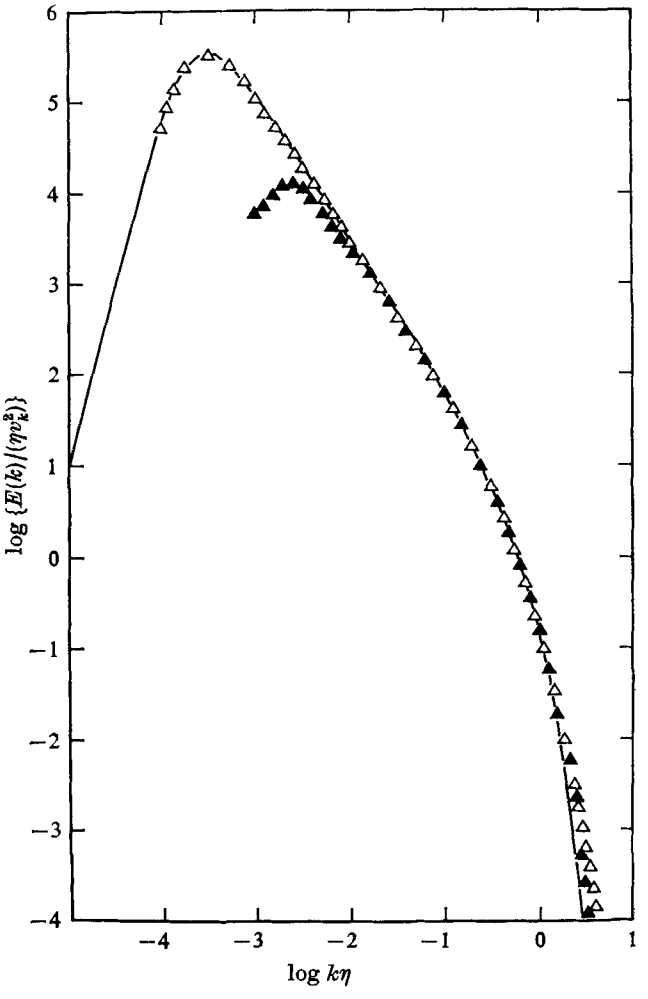

FIGURE 5. Comparison of three-dimensional energy spectra. ▲, CSU grid; △, UCSD jet; ——, von Kármán–Pao spectrum fit to UCSD jet data.

mediate wavenumbers. This is the first time third-order cross-spectra have been used as a test for isotropy. Further calculations of this nature should be made to include the data of Van Atta & Chen (1969). The near antisymmetry of their third-order correlations suggests that better agreement with isotropy may be obtained for their third-order cross-spectra.

The total one-dimensional transfer spectrum $S_{1i,i}$ derived from Im $S_{11,1}$ using (2.13) is compared in figure 4(*b*) with the direct measurement. Agreement is good at the highest wavenumbers with moderate agreement at low and intermediate wavenumbers. The possible influence of the order of data processing operations was carefully checked for this measurement. First, the raw, unsmoothed estimates of Im $S_{11,1}$ and Im $S_{12,2}$ were combined according to (2.11) and then smoothed to form $S_{1i,i}$. Second, the estimates of Im $S_{11,1}$ and Im $S_{12,2}$ were each smoothed and then combined according to (2.11) to form $S_{1i,i}$. The two one-dimensional total

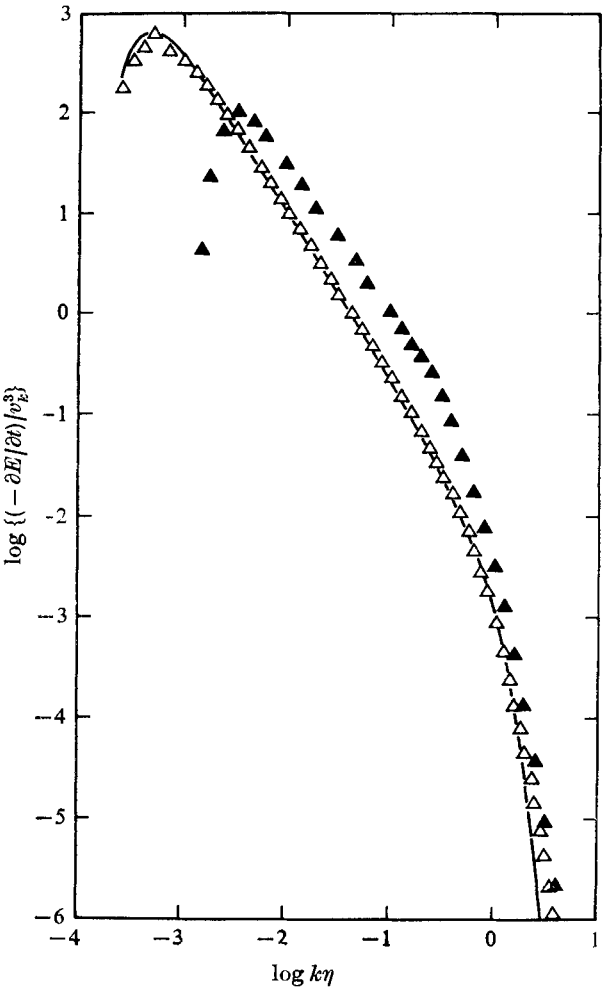

FIGURE 6. Comparison of three-dimensional energy decay spectra calculated assuming local self-preservation. ▲, CSU grid; △, UCSD jet; ——, von Kármán–Pao spectrum fit to UCSD jet data.

transfer spectra were in excellent agreement, and only the first case is shown in figure 4 (*b*). This is an important check on the consistency of the smoothing operation. The one-dimensional transfer spectra $S_{1i,i}$ and Im $S_{11,1}$ were both used to determine three-dimensional transfer spectra so that an estimate could be made of the sensitivityof T to small differences in the one-dimensional transfer spectra.

Three-dimensional spectra

The three-dimensional energy spectrum derived from the one-dimensional total energy spectrum and (2.2) is shown in figure 5. The three-dimensional energy decay spectrum determined from the approximation of local self-preservation is presented in figure 6. The directly measured three-dimensional energy transfer spectra derived from the one-dimensional transfer spectra using (2.10) are

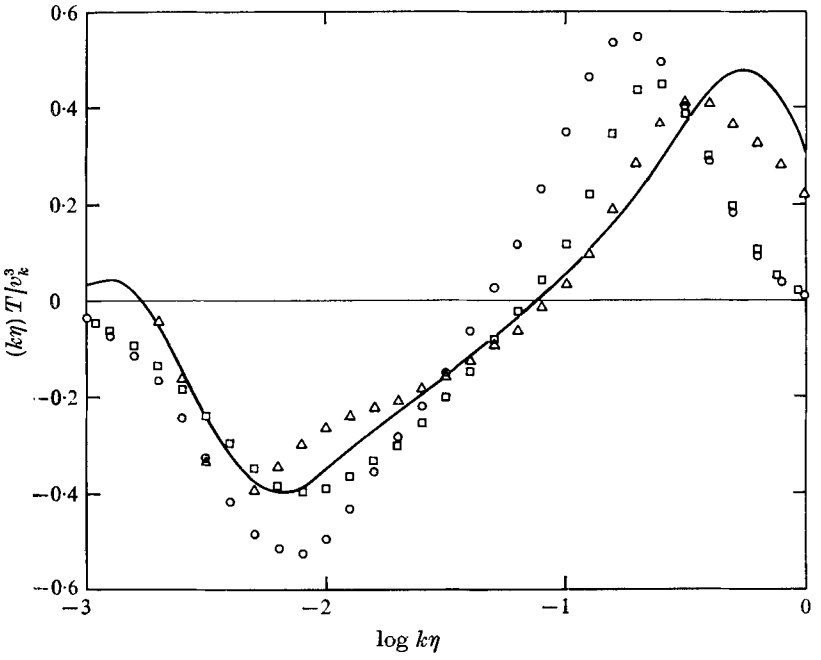

FIGURE 7. Comparison of three-dimensional energy transfer spectra for CSU grid. Direct estimates: ○, from Im $\{k_1^2 S_{11,1}\}$; □, from $k_1^2 S_{1i,i}$. Indirect estimates with local self-preservation: △, from measured energy spectrum; ——, from empirical von Kármán–Pao energy spectrum.

compared in figure 7 with the indirectly measured transfer spectrum derived from (2.1). The two directly measured transfer spectra are in good agreement at high and low wavenumbers but differ at the intermediate wavenumbers. This behaviour is consistent with the differences observed in $S_{1i,i}$ in figure 4(*b*). The indirectly calculated transfer spectrum derived from the local self-preservation approximation is in fair agreement with the direct measurements at low and intermediate wavenumbers. These two measurements become significantly different for $\log k\eta > -0{\cdot}5$. The disagreement at large wavenumbers might indicate a limitation of the self-preservation approximation, distortion due to wire-length effects, lack of isotropy or a combination of all three. It is not possible with the present data to determine the source of the disagreement between the direct estimate and the self-preservation prediction. However, considering the limitations of the CSU grid data, the agreement at low and intermediate wavenumbers suggests that we have successfully determined most of the three-dimensional energy transfer spectrum at a moderately high Reynolds number.

5. Experimental results for UCSD jet

One-dimensional spectra

The measured one-dimensional third-order cross-spectrum $S_{11,1}$ is shown in figure 8. The real part should be small if the jet flow is isotropic, but the real part of the measured spectrum is about an order of magnitude larger than the

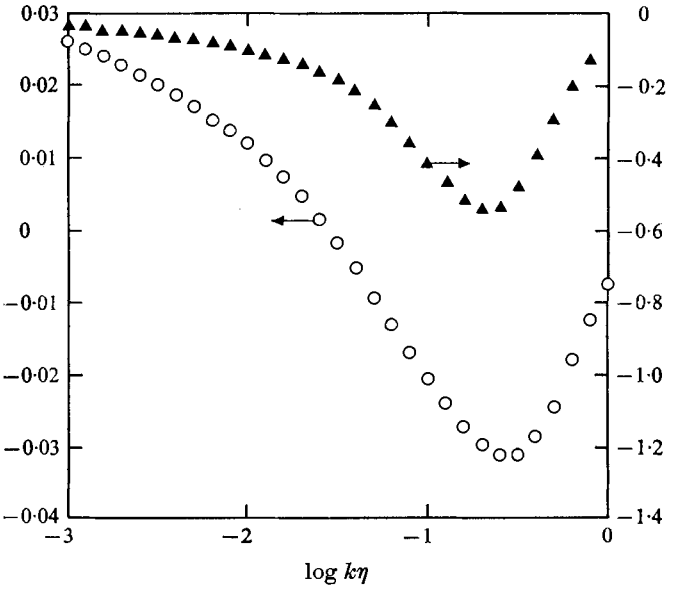

FIGURE 8. One-dimensional complex third-order spectrum $(k_1\eta)^2 S_{11,1}/(v_k^3/\eta)$ of longitudinal velocity for USCD jet measurements. ○, imaginary part; ▲, real part.

imaginary part. For comparison, the real parts of the third-order spectra for the CSU grid data in figure 3 are about the same magnitude as their corresponding imaginary parts. This suggests that the approach to isotropy by the grid turbulence is closer than that for the jet turbulence. It should be emphasized, however, that at present we can only use the magnitude of the real part of the third-order spectrum as a qualitative indication of the approach to isotropy. It is not clear how small the real part of the third-order spectrum must be in order to make isotropy a reasonable approximation in the calculation of the third-order energy transfer spectrum $T(k)$. Additional experimental work in flows with varying degrees of anisotropy is needed before quantitative conclusions will be possible.

Three-dimensional spectra

The three-dimensional energy spectrum $E(k)$ derived from the one-dimensional energy spectrum ϕ_{ii} is compared in figure 5 with the CSU grid spectrum. The local self-preservation approximation to the one-dimensional total energy decay spectrum was used to determine the three-dimensional energy decay spectrum shown in figure 6. Finally, the indirectly measured three-dimensional transfer spectrum for the UCSD jet is compared in figure 9 with the directly measured transfer spectrum.

The agreement between the measured energy transfer spectrum and the self-preservation estimate is remarkably good at intermediate wavenumbers but deteriorates at the highest wavenumbers. The agreement may be fortuitous in view of the number of possible causes of disagreement. These include failures of the approximation of local self-preservation or Taylor's hypothesis in high

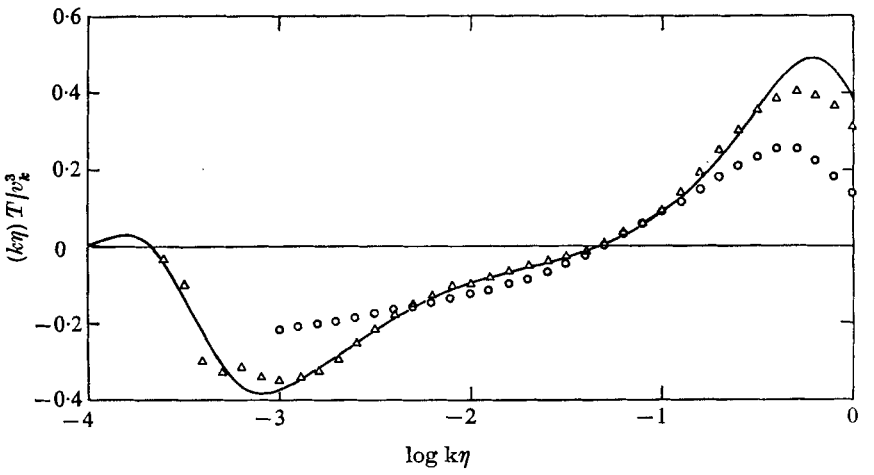

FIGURE 9. Comparison of three-dimensional energy transfer spectra for UCSD jet. ○, direct estimate from Im $\{k_1^2 S_{11,1}\}$. Indirect estimate with local self-preservation: △, from measured energy spectrum; ——, from empirical von Kármán-Pao energy spectrum.

intensity turbulence and lack of isotropy. The energy-spectrum test for isotropy used in the analysis of the CSU grid data is not possible for the UCSD jet as only one component of the velocity was measured. Few such investigations have been made on the validity of isotropy in turbulent jets, and the results are conflicting. In particular, the measurements of ϕ_{11} and ϕ_{22} by Gibson (1963) in a high Reynolds number axisymmetric jet show good agreement with isotropy at wavenumbers $\log k\eta > -2{\cdot}8$, but unpublished measurements of a similar energy-spectrum test of isotropy by Champagne (private communication) in an axisymmetric jet show agreement at second order with isotropy only for $\log k_1\eta > -1{\cdot}2$. The calculation of the energy transfer spectrum by direct and indirect methods provides the only spectrally selective test of isotropy possible with only the measurement of the longitudinal velocity component available from the UCSD jet data. The early measurements of the shear correlation coefficient for a narrow band of frequencies by Corrsin & Uberoi (1951) show a trend consistent with local isotropy at high wavenumbers (or frequencies). The frequency-dependent shear correlation is related to the coherence measurement discussed previously. Unfortunately their measurements did not include both the longitudinal and the radial energy spectra so it is not possible to determine how small the shear coefficient (or coherence) must be to obtain good agreement in the energy-spectra test for isotropy. Other measurements in the UCSD jet with heat addition reported by McConnell (1976) on the statistics of the temperature derivative show marked deviations from isotropy with the skewness $S(d\theta/dt)$ of the temperature derivative of order one.

6. Reynolds number variation of the energy transfer spectra

The energy transfer spectra are compared in figure 10 for a wide range of the turbulent Reynolds number R_λ. Three transfer spectra, with $R_\lambda = 35$, 237 and 951, from Yeh & Van Atta (1973), the CSU grid measurements and the UCSD jet

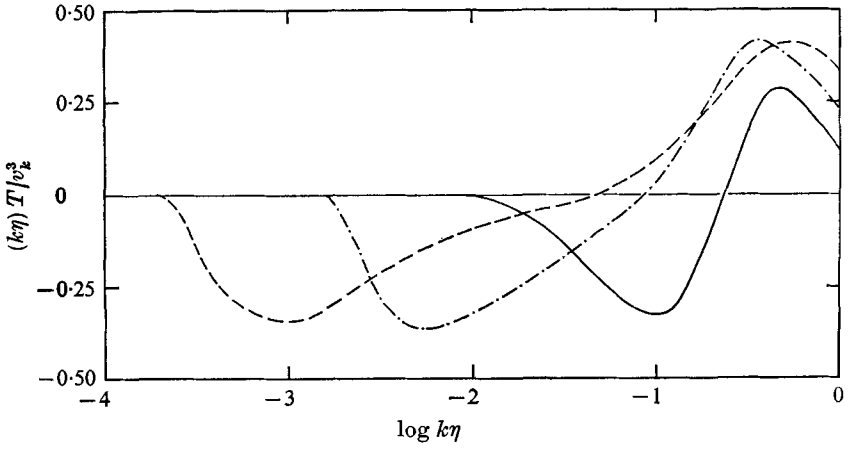

FIGURE 10. Reynolds number variation of three-dimensional energy transfer spectra for $35 < R_\lambda < 951$. ——, $R_\lambda = 35$, Yeh & Van Atta (1973); —·—, $R_\lambda = 237$, CSU grid; – – –, $R_\lambda = 951$, UCSD jet.

measurements respectively are included. There is a rough clustering of the high wavenumber tails of the transfer spectra, but they do not appear to collapse onto each other at these wavenumbers as one might expect. The Reynolds number effects are readily apparent at low and intermediate wavenumbers. The negative peak retains nearly the same shape and magnitude but shifts uniformly to lower wavenumbers as the Reynolds number increases. Kolmogorov scaling should not be expected to collapse the lower wavenumber data. An alternative scaling using the external velocity and length scales suggested by the measurements of Uberoi (1963) would tend to collapse the low wavenumber parts of the transfer spectra.

The form of the energy transfer spectrum at intermediate wavenumbers (bounded by the location of the positive and negative peaks of kT) tends towards $kT \approx 0$ over a range of wavenumbers as R_λ increases. It has been suggested (see Uberoi, for instance) that the inertial subrange corresponds to the wavenumber domain for which T (or kT) is identically zero. This notion of an inertial subrange has at times been used synonymously with $E \sim k^{-\frac{5}{3}}$ behaviour of the energy spectrum, but the data presented in figure 5 suggest otherwise. The UCSD jet energy spectrum in figure 5 has a nearly $k^{-\frac{5}{3}}$ range over a decade of wavenumbers, but the energy transfer spectrum in figure 9 shows no corresponding range of wavenumbers over which kT is nearly zero (except for the zero-crossing). It may be that the existence of a range of wavenumbers over which $T \equiv 0$ is a sufficient condition for an extensive $k^{-\frac{5}{3}}$ range in the energy spectrum, but the converse is apparently not valid.

7. Extrapolation to high Reynolds number flows

Empirical method

Measurements of the energy transfer spectra in grid turbulence at Reynolds numbers R_λ exceeding 10^3 or numerical or theoretical efforts which are capable of predicting the transfer spectra at such Reynolds numbers are not likely to be

available in the near future. Empirical estimates are never an entirely satisfactory substitute for either theoretical or experimental results, but with only a few modest assumptions predictions for the energy transfer spectrum $T(k)$ can be obtained which are remarkably close to the transfer spectra derived from measurements at moderate Reynolds number. We shall see that the predictions for moderate Reynolds number are not only qualitatively similar to the measurements but are generally in adequate quantitative agreement as well. Considering the difficulty and expense of performing such experiments at higher Reynolds numbers, the empirical method for extrapolating the measurements at lower Reynolds numbers is worth trying.

An interpolation formula for the three-dimensional energy spectrum was suggested by von Kármán (1948) as an empirical representation which would both describe available measurements and be easy to manipulate mathematically. The formula

$$E(k)/v_k^2\eta = \alpha(L/\eta)^{\frac{5}{3}}(kL)^4[1+(kL)^2]^{-\frac{17}{6}} \tag{7.1}$$

is chosen to have $E \sim k^{-\frac{5}{3}}$ for large k and $E \sim k^4$ for small k. L is the 'energy' scale and α is the Kolmogorov constant. The constant α in (7.1) has been evaluated by matching the spectral behaviour to the inertial subrange so that $E = \alpha\epsilon^{\frac{2}{3}}k^{-\frac{5}{3}}$.

The von Kármán formula does not describe the exponential-like cut-off of the energy spectrum at dissipation-scale wavenumbers ($k\eta = O(1)$, say). The high wavenumbers can be roughly approximated by closure models having origins in suggestions of Onsager (1949) and Corrsin (1964) and applied to velocity spectra by Pao (1965). They derived formulae for $E(k)$ by setting $\partial E/\partial t$ to zero for wavenumbers in the inertial subrange and larger, i.e. $T(k) = 2\nu k^2 E(k)$ for $k \gg 1/L$, where $1/L$ is the wavenumber characterizing the energy scale. The transfer term $T(k)$ is related to E by a closure model, and E is obtained for $k \gg 1/L$. The spectral form of Pao, given by

$$E(k)/v_k^2\eta = \alpha(k\eta)^{-\frac{5}{3}}\exp[-\tfrac{3}{2}\alpha(k\eta)^{\frac{4}{3}}], \tag{7.2}$$

was used to approximate the largest wavenumbers. Other representations for the dissipation wavenumbers of the energy spectrum are possible, but for the present purposes only minor differences result since we are primarily interested in the behaviour of $T(k)$ at low and intermediate wavenumbers.

The three-dimensional energy spectrum for all wavenumbers is approximated by the combination of (7.1) and (7.2)

$$E(k;\, L;\, \beta)/v_k^2\eta = \alpha(L/\eta)^{\frac{5}{3}}(kL)^4[1+(kL)^2]^{-\frac{17}{6}}\exp[-\tfrac{3}{2}\beta(k\eta)^{\frac{4}{3}}], \tag{7.3}$$

where the parameter $\beta \approx \alpha$ has been substituted for α in the exponential term of the Pao spectrum. The parameter β is determined by satisfying the dissipation constraint

$$\int_0^\infty 2\nu k^2 E(k)\, dk = \epsilon. \tag{7.4}$$

Since experimental results herein suggest that self-preservation can provide a useful approximation to the energy decay spectrum at low to moderate

Reynolds numbers, the assumption of self-preservation was applied to the empirical energy spectrum to estimate energy transfer spectra at high Reynolds numbers.

Comparison with measurements

The empirical spectrum was fitted to the CSU grid and UCSD jet data by suitable choice of the parameter α and scale ratio L/η. The empirical spectrum and the UCSD jet data are compared in figure 5. The spectra are in reasonable agreement over most of the wavenumber range but are in poor agreement at high wavenumber. The measured and empirical three-dimensional energy decay spectra for the jet data are shown in figure 6. It should be noted that, since both the empirical and the 'measured' decay spectra were determined using the approximation of local self-preservation, figure 6 represents an alternative test of how well the empirical energy spectrum fits the data. The empirical predictions for the energy transfer spectra for the CSU grid data and the UCSD jet data are shown in figures 7 and 9 respectively. The agreement is good in the low to moderate wavenumber range, but the empirical predictions of the energy transfer spectra deviate significantly for both the grid and jet data at high wavenumber. This result is consistent with the quality of the fit between measured and empirical energy spectra. We assume that the low Reynolds number measurements of the energy transfer spectrum have defined the high wavenumber portion of the transfer spectrum. It is the low and intermediate wavenumber range of the transfer spectrum which is difficult to measure at large Reynolds number. The good agreement between the direct measurement and the empirical prediction for the energy transfer spectra supports the utility of both the von Kármán–Pao spectrum and the approximation of local self-preservation.

Energy transfer spectrum and the inertial subrange

The energy transfer spectra for $10^2 \leqslant R_\lambda \leqslant 10^5$ are shown in figure 11. Kolmogorov variables provide approximately universal scaling only at the highest wavenumbers; this is a result of the inability of Kolmogorov variables to scale the energy decay spectrum, and the transfer spectrum scaled with Kolmogorov variables can become universal only at large wavenumbers where $\partial E/\partial t \ll D$.

Our purpose here is to relate the predictions for the Reynolds number variation of the transfer spectrum to conditions defining the existence of an inertial subrange. Bradshaw (1967) has considered numerous attempts made to specify the conditions for the existence of an inertial subrange. He suggests that a necessary condition is that the energy transfer through a wavenumber k in the inertial subrange must be nearly equal to the total dissipation. Alternatively, Uberoi (1963) has implied in a sketch that the net energy transfer spectrum must be nearly zero to obtain an inertial subrange. These criteria for the inertial subrange can be examined using the present estimates for the energy transfer spectra at high Reynolds number.

The presentation of T in figure 11 multiplied by k does not show clearly whether or not the energy transfer spectrum itself approaches zero in the inertial subrange, but even for $R_\lambda = 10^4$–10^5, the transfer function has no region where $T \approx 0$

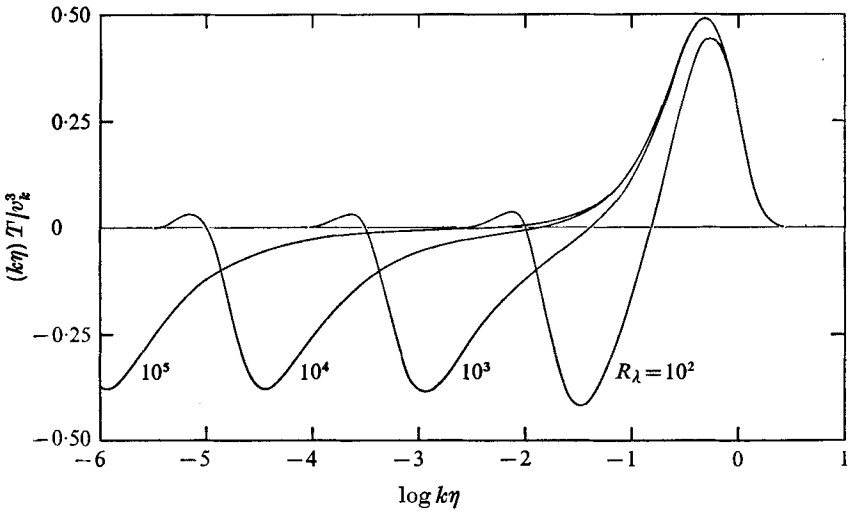

FIGURE 11. Empirical three-dimensional energy transfer spectra calculated indirectly.

despite the extensive inertial subrange ($E \sim k^{-\frac{5}{3}}$) at these high Reynolds numbers. This suggests that $T \approx 0$ is a sufficient but not a necessary condition for the existence of an inertial subrange.

A criterion due to Lumley (1964) provides a more suitable bound for the wavenumber range of the inertial subrange which is approximately coincident with the extent of the $k^{-\frac{5}{3}}$ region of the energy spectrum. Define the spectral energy flux by

$$S(k) = -\int_0^k T(k)\,dk, \tag{7.5}$$

where $S(k)$ represents the energy flux from wavenumbers below k to wavenumbers above k. The inertial subrange is characterized by constant spectral energy flux or, equivalently, a region where the energy transfer T is identically zero. A region of non-constant spectral energy flux might be expected to introduce other parameters into the inertial-subrange formulation in contradiction to the requirement which permits dependence on ϵ and k alone. As Lumley points out, there are two assumptions implied here: first, the energy spectrum is determined by the spectral energy flux, and second, the energy flux is a constant. Lumley suggests that the requirement of constant spectral flux in the inertial subrange may be too stringent, and the second of the two assumptions above should be relaxed to $S(k)$ 'nearly constant'. If the net transfer into or out of the energy spectrum is sufficiently small in comparison with the spectral flux, the inertial subrange is at most weakly affected by the small variations in the spectral flux. More specifically, since the quantity $|S/(dS/dk)|$ is a measure of the wavenumber increment Δk over which S varies significantly, comparison of Δk with the local wavenumber through the ratio $|k/\Delta k|$ provides a criterion for the wavenumber region of nearly constant spectral energy flux.

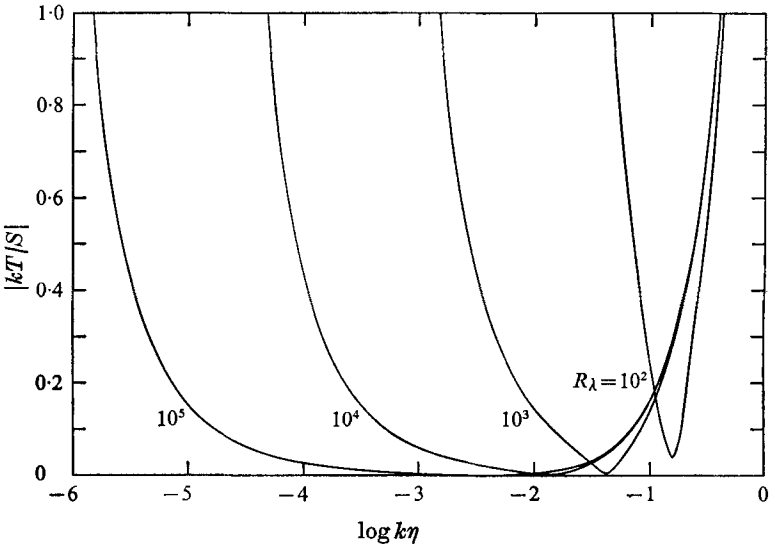

FIGURE 12. The inertial-subrange criterion due to Lumley (1964) calculated for the von Kármán–Pao empirical energy transfer model.

The Lumley criterion $|kT/S|$ applied to the empirical system is shown in figure 12. The wavenumber range over which $|kT/S| \ll 1$ corresponds roughly to the $k^{-\frac{5}{3}}$ range of the empirical energy spectrum. There is qualitative agreement between $|kT/S| \ll 1$ and inertial-subrange-type behaviour, but it is impossible to select a unique value of the ratio $|kT/S|$ which strictly delineates the extent of the inertial subrange; separate values of the criterion are required to define the low and high wavenumber extent of the inertial subrange. While a precise value cannot be given, $|kT/S| < 0{\cdot}1$ provides an approximate criterion for the existence of an inertial subrange for $R_\lambda > 10^3$ in this model system. It is clear, however, that the criterion of Lumley provides a more satisfactory condition for the existence of an inertial subrange than the strict requirement of $S(k) \equiv$ constant (or $T \equiv 0$).

8. Concluding remarks

Our purpose in this investigation has been to determine the variation with Reynolds number of the three-dimensional transfer spectrum. We were able to extend the measurements of $T(k)$ to Reynolds numbers about an order of magnitude larger than those previously available, and by using an empirical extrapolation with only mild assumptions, we were able to extend the estimates of $T(k)$ to some of the highest Reynolds numbers of interest, comparable with the turbulent Reynolds numbers observed in atmospheric measurements. An extrapolation of this kind cannot be accepted without caution, but the quality of the agreement between the empirical model and the measurements at lower Reynolds numbers suggests that errors in estimates for the higher Reynolds numbers are probably not significant. The measurements and the extrapolations

show that the inertial subrange is roughly coincident with small $kT(k)$ instead of some earlier notions that $T(k)$ itself must be small. These results are consistent with the 'nearly constant flux' arguments of Lumley (1964).

Measurements of the net energy transfer spectrum $T(k)$ do not provide information on the relative interaction among different wavenumbers. It would be valuable to determine the transfer spectrum $T(k, k')$, which represents the net transfer between two spherical wavenumber shells with radii k and k'. The measurement of $T(k, k')$ is at least theoretically possible with present hot-wire techniques, but it is clear that the experimental effort required is exceedingly large and does not appear justified at this time. Significant questions also remain to be answered on the kind of third-order measurements employed in the present investigation.

The data used herein are not the most suitable available for examining the interesting question of testing the existence of isotropy with third-order spectral techniques. We are at present re-examining the data of Van Atta & Chen (1969) to investigate the third-order isotropy criterion specified by (2.13). In addition, we plan to examine more closely the question of statistical convergence of the third-order cross-spectrum. The rate of convergence for third-order quantities is slow, and there is a need for variance estimation techniques for analysing third-order spectra. Third-order spectral measurements of this kind in a shear flow would provide an important contrast to grid-turbulence measurements. Shear-flow data would assist in interpreting the relative approach to local isotropy in a flow which does not produce nearly isotropic conditions at all wavenumbers. The limited jet data analysed herein suggest that dramatic differences would be observed among third-order spectra measured in shear and grid flows.

We wish to thank Dr C. A. Friehe for the use of the large Reynolds number jet data, and Dr T. T. Yeh for discussions and help with the analysis and computing. The research was supported by National Science Foundation Grants GK-43643X and ENG74-02229 and by the Office of Naval Research under Contract N00014-76-C-0702. This work forms part of the Ph.D. thesis of K. N. Helland (1974).

REFERENCES

BATCHELOR, G. K. 1953 *The Theory of Homogeneous Turbulence.* Cambridge University Press.

BRADSHAW, P. 1967 Conditions for the existence of an inertial subrange in turbulent flow. *Nat. Phys. Lab. Aero. Rep.* no. 1220.

CORRSIN, S. 1964 Further generalizations of Onsager's cascade model for turbulent spectra. *Phys. Fluids*, **7**, 1156.

CORRSIN, S. & UBEROI, M. S. 1951 Spectra and diffusion in a round turbulent jet. *N.A.C.A. Tech. Note*, no. 1040.

FAVRE, A., GAVIGLIO, J. & DUMAS, R. 1955 Some measurements of time and space correlation in wind tunnel. *N.A.C.A. Tech. Memo.* no. 1370.

GIBSON, M. M. 1963 Spectra of turbulence in a round jet. *J. Fluid Mech.* **15**, 161.

HELLAND, K. N. 1974 Energy transfer in high Reynolds number turbulence. Ph.D. thesis, University of California, San Diego.

HINZE, J. O. 1959 *Turbulence.* McGraw-Hill.

KÁRMÁN, T. VON 1948 Progress in the statistical theory of turbulence. *J. Mar. Res.* **7**, 252.

KISTLER, A. L. & VREBALOVICH, T. 1966 Grid turbulence at large Reynolds numbers. *J. Fluid Mech.* **26**, 37.

LUMLEY, J. L. 1964 The spectrum of nearly inertial turbulence in a stably stratified fluid. *Phys. Fluids*, **21**, 99.

MCCONNELL, S. O. 1976 The fine structure of velocity and temperature measured in the laboratory and the atmospheric marine boundary layer. Ph.D. thesis, University of California, San Diego.

ONSAGER, L. 1949 Statistical hydrodynamics. *Nuovo Cimento. Suppl.* **6**, 279.

PAO, Y. H. 1965 Structure of turbulent velocity and scalar fields at large wavenumbers. *Phys. Fluids*, **8**, 1063.

PIERCE, R. E. 1972 Statistical analysis of turbulence using a large scale digital computing system. Ph.D. thesis, The Pennsylvania State University.

SCHEDVIN, J., STEGEN, G. R. & GIBSON, C. H. 1974 Universal similarity at high grid Reynolds numbers. *J. Fluid Mech.* **65**, 561.

STEGEN, G. R. & VAN ATTA, C. W. 1970 Phase speed measurements in grid turbulence. *J. Fluid Mech.* **42**, 689.

UBEROI, M. S. 1963 Energy transfer in isotropic turbulence. *Phys. Fluids*, **6**, 1048.

VAN ATTA, C. W. & CHEN, W. Y. 1969 Measurements of spectral energy transfer in grid turbulence. *J. Fluid Mech.* **38**, 743.

YEH, T. T. & VAN ATTA, C. W. 1973 Spectral transfer of scalar and velocity fields in heated-grid turbulence. *J. Fluid Mech.* **58**, 233.